Supplementary Information: Thermal phase design of ultrathin magnetic iron oxide films: From Fe_3O_4 to γ-Fe_2O_3 and FeO

Mai Hussein Hamed,[ab] David N. Mueller,[a] and Martina Müller[*ac]

1 Characterization of structural and magnetic properties

We grow a series of ultrathin magnetite Fe_3O_4 films, i.e. 2 nm, 4 nm and 38 nm on two different oxide substrates, $SrTiO_3$ (001) and yttria-stabilized zirconia (001) (YSZ). We characterized the heterostructures using different techniques, and present the X-ray diffraction (XRD) and magnetic measurements via vibrating sample magnetometry (VSM) in the following.

Fig. 1 (a) and (c) show the XRD pattern of Fe_3O_4 38 nm thick films grown on $SrTiO_3$ and YSZ, respectively. The XRD pattern in Fig. 1 (a) confirms the epitaxial growth of Fe_3O_4 (100) on $SrTiO_3$ (100). In Fig. 1 (c) the growth of Fe_3O_4 (111) on YSZ (100) reveals the formation of fringes which refer to a high quality of the crystalline structure of the magnetite film.

A clear indication for the stoichiometric quality of the magnetite thin films is by determining the Verwey temperature T_V. Fig. 1 (b) and (d) show the magnetization vs. temperature (M(T)) curves of Fe_3O_4 38 nm thick films grown on $SrTiO_3$ and YSZ, respectively. In particular, the first and second derivatives of the magnetization curves is utilized to determine T_V and the transition width ΔT_V. The curves show a strong decrease for the magnetization around 120 K referring to the Verwey transition. This observation thereby confirms the stoichiometry of the magnetite thin films.

After optimizing the growth parameters and confirming the high quality of the 38 nm thick Fe_3O_4 films by the different characterization methods grown on $SrTiO_3$ (for more details see our previous work[1]) and on YSZ, also ultrathin films of 2 nm and 4 nm are grown on both $SrTiO_3$ and YSZ substrates.

2 HAXPES

In order to ensure that the kinetics of the thermal annealing experiment is not playing a role for our analysis, we performed the following test experiments: We annealed a film of 4 nm at 600 °C in UHV for 90 min, and took HAXPES spectra every 30 min. No changes occur in the spectra as depicted in Fig. 2.

All HAXPES have been analyzed quantitatively by a linear combination fitting of the elemental spectral weights, as shown in Fig. 3(a) and (b). In particular, we calculate the Fe, Fe^{2+} and Fe^{3+} cation ratios with respect to the annealing temperature, and thereby conclude on the chemical phase ratio.

To exclude any cations diffusion, we conducted HAXPES to a 38 nm thick film grown on $SrTiO_3$ substrate. Figure 4 shows the survey spectra of the films annealed at different temperature up to 700 °C in comparison to Fe 2p core level spectra of $SrTiO_3$ substrate as a reference for possible cations diffusion from the underlying substrate.

## 3 Thermodynamics calculations

Under thermal annealing, the iron oxide films undergo transitions into different chemcial phases, for which the three equilibrium equations are given below:

$$① \ 3Fe_2O_3 \rightleftharpoons 2Fe_3O_4 + \frac{1}{2}O_2 \tag{1}$$

$$② \ Fe_3O_4 \rightleftharpoons 3FeO + \frac{1}{2}O_2 \tag{2}$$

$$③ \ FeO \rightleftharpoons Fe + \frac{1}{2}O_2. \tag{3}$$

[a] Peter-Grünberg-Institut (PGI-6), Forschungszentrum Jülich GmbH, 52425 Jülich, Germany; E-mail: mart.mueller@fz-juelich.de

[b] Faculty of Science, Helwan University, 11795 Cairo, Egypt.

[c] Experimentelle Physik I, Technische Universität Dortmund, 44227 Dortmund, Germany.
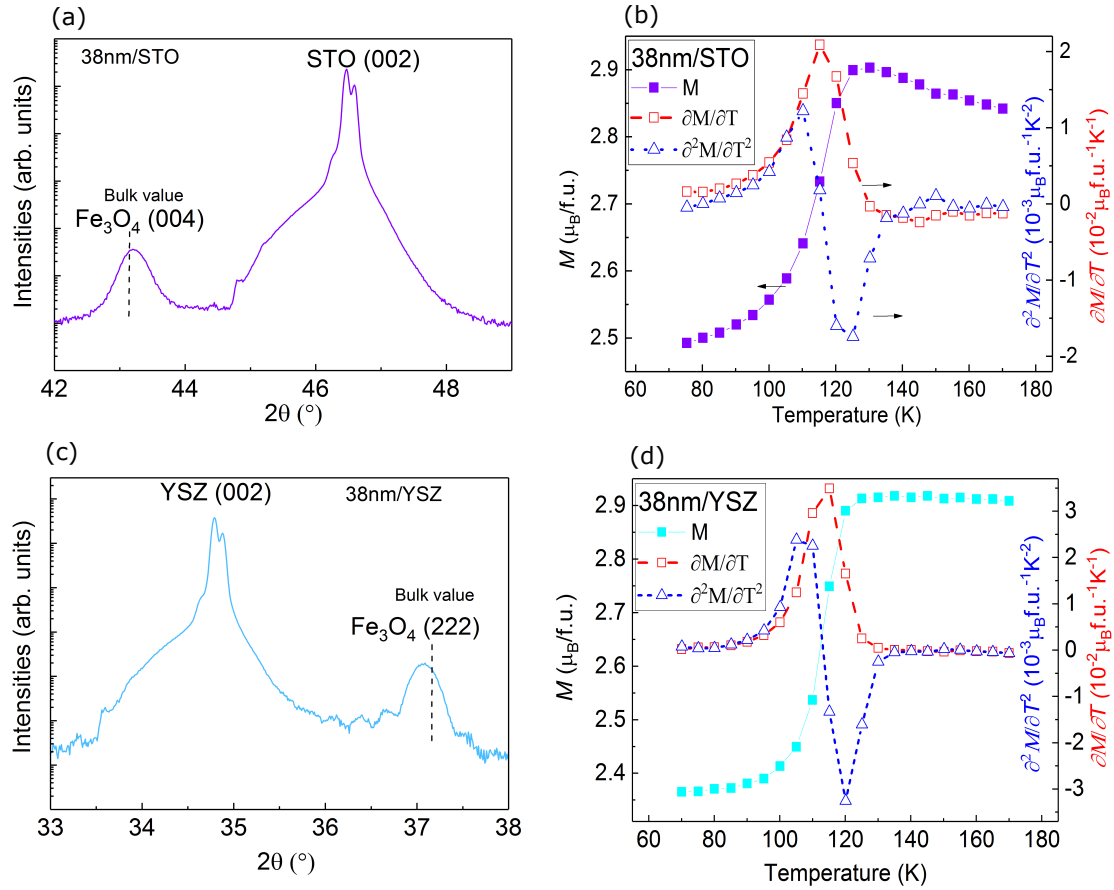
Fig. 1 (a) and (c) Out-of-plane x-ray diffraction θ-2θ-scans of the Fe_3O_4 (004)/$SrTiO_3$ (002) and the Fe_3O_4 (222)/YSZ (002) reflections, respectively for films 38 nm thick. (b)[1] and (d) Magnetic detection of Verwey transition of 38 nm thick film: $M(T)$, the first and second derivatives for the magnetization curve to detect T_V and ΔT_V of films grown on $SrTiO_3$ and YSZ, respectively.
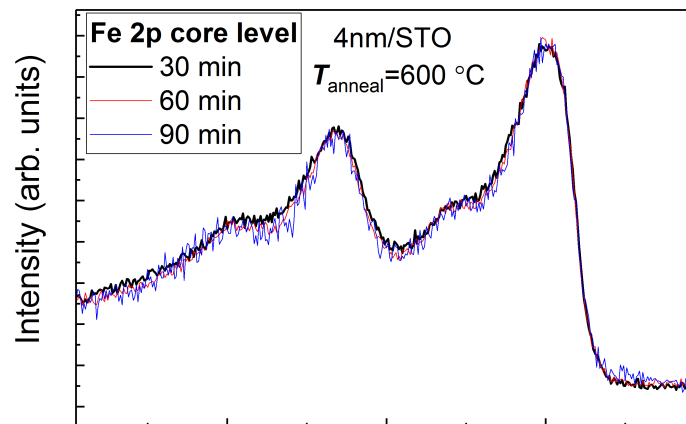
Fig. 2 Fe 2p core level HAXPES spectra for 4nm/STO films annealed at 600 °C in UHV for 30, 60 and 90 min.
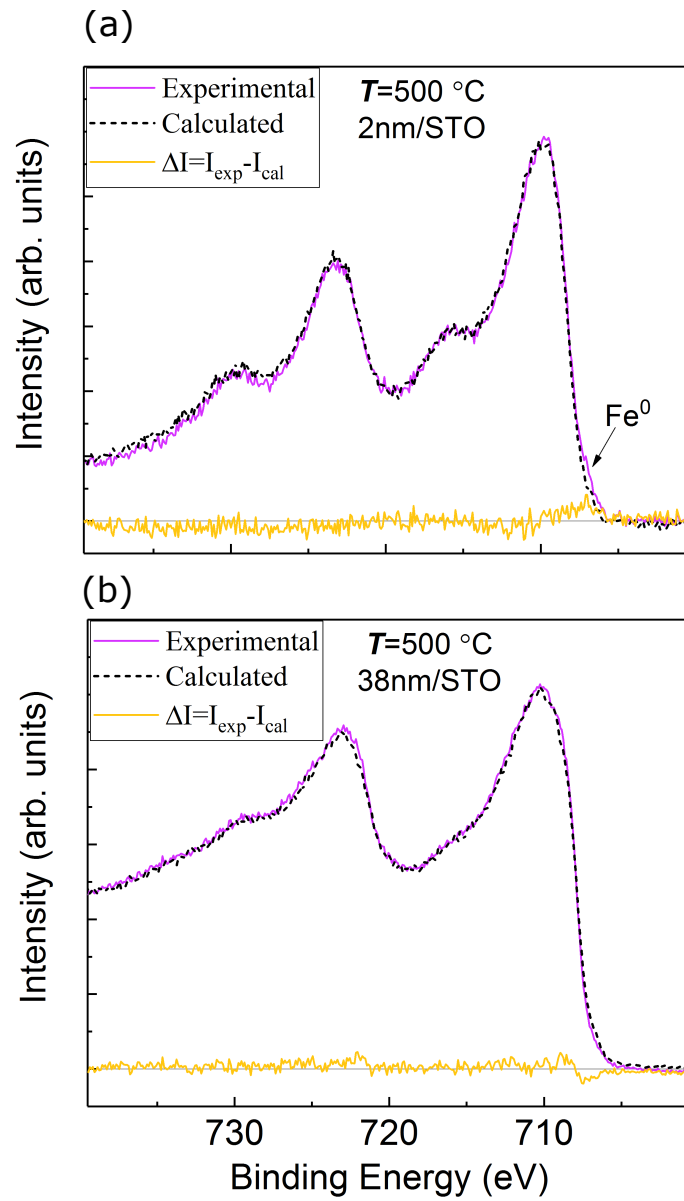
**Fig. 3** (a) and (b) Fitting example for films annealed at $500\,°C$ of thickness $2\,nm$ and $38\,nm$, respectively.
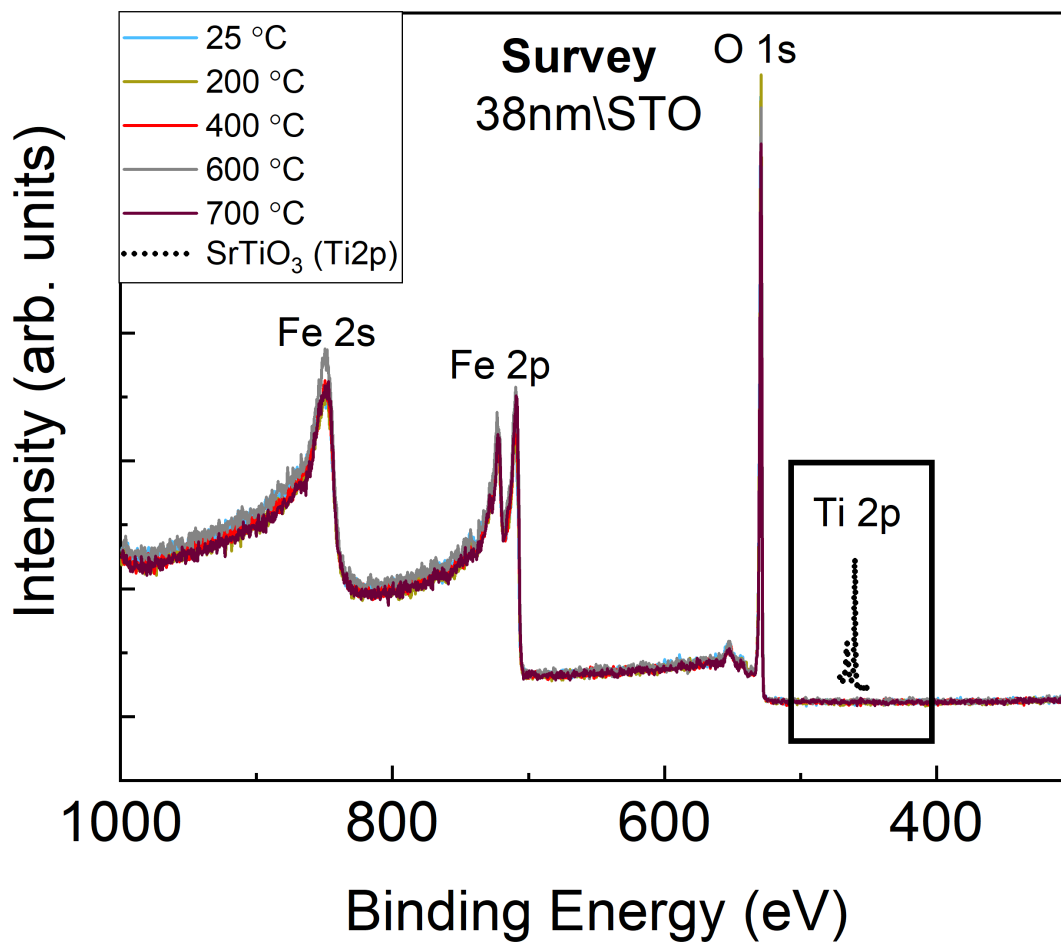
Fig. 4 Survey spectra for $38\,\mathrm{nm}$ film grown on $SrTiO_3$ substrate annealed in different temperature. In doted line, a Ti 2p core level spectra of $SrTiO_3$ substrate.

The classical van 't Hoff analysis for the phase equilbria reads as

$$\ln(K) = -\frac{\Delta G^0}{RT} = -\frac{\Delta H}{RT} + \frac{\Delta S}{R}, \tag{4}$$

whereby R is the gas constant, ΔG^0 is the change of Gibbs free energy, ΔH is the change of the enthalpy and ΔS of the entropy. K the equilibrium constant of the equilibria according to 1, 2 and 3, respectively. K is directly related to the Fe, Fe^{2+} and Fe^{3+} cation ratios as shown below, which we determined from the HAXPES peak fitting analysis.
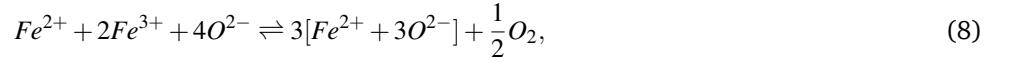
From the first equilibirium 1,

$$3[2Fe^{3+} + 3O^{2-}] \rightleftharpoons 2[Fe^{2+} + 2Fe^{3+} + 4O^{2-}] + \frac{1}{2}O_2, \tag{5}$$
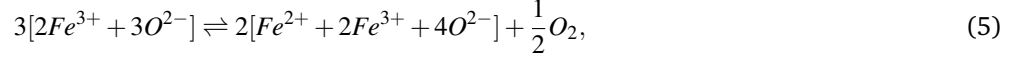
we derive

$$K_① = \frac{[Fe^{3+}]^4 [Fe^{2+}]^2 [O^{2-}]^8}{[Fe^{3+}]^6 [O^{2-}]^9} p_{O_2eff}^{\frac{1}{2}}, \tag{6}$$

where, p_{O_2eff} is the effective oxygen pressure p_{O_2eff} of the heterostructure, i.e substrate, film and atmosphere. We reorganize the equation to

$$K_① = \left[\frac{Fe^{2+}}{Fe^{3+}}\right]^2 p_{O_2eff}^{\frac{1}{2}} = K_{red①} \times p_{O_2eff}^{\frac{1}{2}}. \tag{7}$$

For the second equilibirium 2 we derive

$$Fe^{2+} + 2Fe^{3+} + 4O^{2-} \rightleftharpoons 3[Fe^{2+} + 3O^{2-}] + \frac{1}{2}O_2, \tag{8}$$

$$K_② = \frac{[Fe^{2+}]^3 [O^{2-}]^3}{[Fe^{2+}][Fe^{3+}]^2 [O^{2-}]^4} p_{O_2eff}^{\frac{1}{2}}, \tag{9}$$

$$K_② = \left[\frac{Fe^{2+}}{Fe^{3+}}\right]^2 p_{O_2eff}^{\frac{1}{2}} = K_{red②} \times p_{O_2eff}^{\frac{1}{2}}, \tag{10}$$

For the third equilibirium 3 we derive

$$Fe^{2+} + O^{2-} \rightleftharpoons Fe^0 + \frac{1}{2}O_2, \tag{11}$$

$$K_③ = \frac{[Fe^0]}{[Fe^{2+}][O^{2-}]} p_{O_2eff}^{\frac{1}{2}}, \tag{12}$$

$$K_③ = \left[\frac{Fe^0}{Fe^{2+}}\right] p_{O_2eff}^{\frac{1}{2}} = K_{red③} \times p_{O_2eff}^{\frac{1}{2}}, \tag{13}$$

As first approximation we neglect the effective oxygen pressure and calculate K_{red}. Then we calculated the enthalpy (ΔH) and the entropy (ΔS) according to equation 4 for all the samples, as shown in Table 1.

Secondly, we calculated the effective oxygen pressure p_{O_2eff},

$$p_{O_2eff}^{\frac{1}{2}} = \frac{e^{-\frac{\Delta G^0}{RT}}}{K_{red}} \tag{14}$$

with ΔG^0 being a function of temperature. For the three relevant redox processes 1, 2 and 3, we calculated ΔG^0 as follows:

$$\Delta G_①^0(T) = 2G_{Fe_3O_4}^0(T) + \frac{1}{2}G_{O_2}^0 - 3G_{Fe_2O_3}^0(T) \tag{15}$$

$$\Delta G_②^0(T) = 3G_{FeO}^0(T) + \frac{1}{2}G_{O_2}^0 - G_{Fe_3O_4}^0(T), \tag{16}$$

$$\Delta G_③^0(T) = G_{Fe}^0(T) + \frac{1}{2}G_{O_2}^0 - G_{FeO}^0(T). \tag{17}$$

Table 1 Thermodynamics parameters calculated from $ln(K_{red})$ $vs.1/T$.

Film	Reaction	Enthalpy ΔH (kJ/mol)	Entropy ΔS (J/molK)
2 nm/STO	①	35.32±1.9	53.5±4.5
2 nm/STO	②	55.11±6.8	96.2±11.9
2 nm/STO	③	47.19±4.3	42.1±4.7
4 nm/STO	①	25.64±2.1	32.6±4.2
4 nm/STO	②	57.52±22.97	82.5±33.5
4 nm/STO	③	....	....
4 nm/YSZ	①	22.02±3.3	31.1±7.98
4 nm/YSZ	②	53.29±3.9	101.7±7.6
4 nm/YSZ	③	145.8±33.4	176.8±43.1
38 nm/STO	①	....	....
38 nm/STO	②	31.16±2	74.2±3.8
38 nm/STO	③	....	....

$G^0_{Fe_2O_3}(T), G^0_{Fe_3O_4}(T), G^0_{FeO}(T), G^0_{Fe}(T)$ and $G^0_{O_2}$ are calculated from the NIST database[2]. Table 2 shows the standard values of the different iron oxides for the Gibbs formation energy, enthalpy and entropy calculated at room temperature.

Table 2 Standard thermodynamics parameters calculated at room temperature.

	G^0 (kJ/mol)	$\Delta_f H^0$ (kJ/mol)	S^0 (J/molK)
Fe_2O_3	-851.55	-863.21	87.28
Fe_3O_4	-1164.21	-1163.34	145.17
FeO	-290.15	-286.74	60.72
Fe	-20.54	-12.4	27.31

The respective Gibbs formation energy for each equilibrium as function of temperature and the values at room temperature are given in Table 3.

Table 3 The calculated Gibbs formation energy of the three equilbiria at room temperature.

$\Delta G^0_{①}$	$\Delta G^0_{②}$ (kJ/mol)	$\Delta G^0_{③}$
256.996	324.513	300.356

Notes and references

1 M. H. Hamed, R. A. Hinz, P. Lömker, M. Wilhelm, A. Gloskovskii, P. Bencok, C. Schmitz-Antoniak, H. Elnaggar, C. M. Schneider and M. Müller, *ACS Applied Materials & Interfaces*, 2019, **11**, 7576–7583.

2 M. W. Chase, *NIST-JANAF thermochemical tables*, American Institute of Physics for the National Institute of Standards and Technology, U.S. Department of Commerce: Gaithersburg, MD, 4th edn., 1998.